Impact of Renormalization on Order Parameter

GDR QCD 28.09.2023

Nadine Attieh, Nathan Touroux, Marcus Bluhm, Masakiyo Kitazawa, Marlene Nahrgang

QCD phase diagram

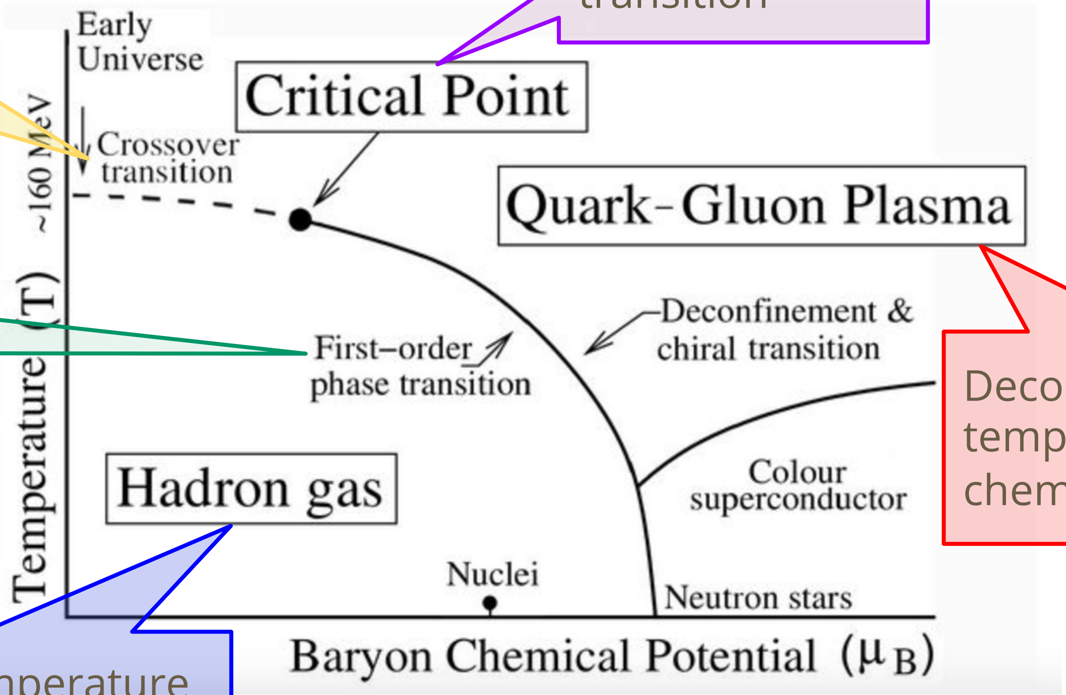

Bhalerao, 1404.3294v1

From lattice QCD

End of 1st order transition

From effective models

Deconfined, high temperature and high chemical potential

Confined, low temperature and low chemical potential

Heavy Ion Collisions

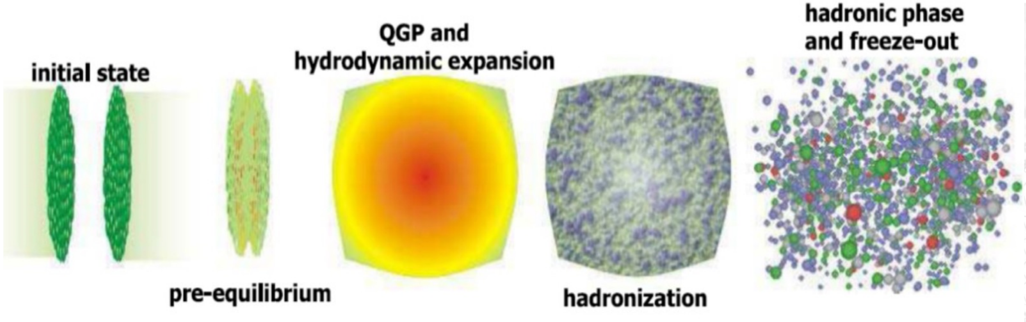

©Silvia Masciocchi GSI Darmstadt and Heidelberg University

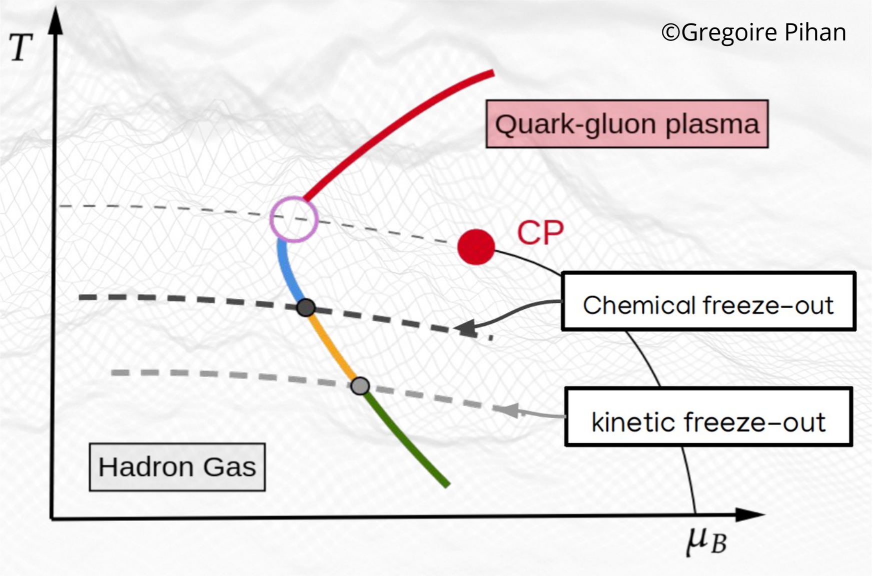

Heavy Ion Collision is highly dynamical

- Short lived
- Small size
- Out of equilibrium evolution

→**Dynamics of fluctuations in HIC**

Can a signal from the critical point survive, and have effects that can be detected after freeze-out?

Fluid dynamics and Fluctuations

Successful at describing the spacetime evolution of systems created in heavy ion collisions

- ➔ Describes QGP-HG phase transition by including an adapted equation of state
- ➔ Current models limited to event-averaged quantities

Describing the impact of fluctuations is important, especially at phase transition; near the critical point, dynamical evolution and critical phenomena intertwine

2 approaches

Deterministic (Hydro+)

Stephanov, Yin 1712.10305
Rajagopal, Ridgway, Weller, Yin 1908.08539
An, Basar, Stephanov, Yee 1902.09517, 1912.13456
Pradeep, Rajagopal, Stephanov, Yin 2204.00639

Stochastic Fluid Dynamics

Challenge: lattice spacing dependence introduced by noise

Chiral Fluid Dynamics

Couple fluid dynamic evolution of fireball to fluctuations of chiral order parameter

$$\frac{\partial^2 \varphi(\vec{x},t)}{\partial t^2} - \nabla^2 \varphi(\vec{x},t) + \eta \frac{\partial \varphi(\vec{x},t)}{\partial t} + \frac{\partial V_{\text{eff}}[\varphi]}{\partial \varphi(\vec{x},t)} = \boxed{\xi(\vec{x},t)}$$

noise

$$\partial_\mu T^{\mu\nu} = -\partial_\mu T^{\mu\nu}_{\varphi}$$

Large dip in kurtosis of net-proton number on expected crossover side of critical point

Herold, Nahrgang, Yan and Kobdaj 1601.04839v1
Nahrgang, Leupold, Herold, Bleicher 1105.0622
Bluhm, Jiang, Nahrgang, Pawlowski, Rennecke, Wink 1808.01377v1

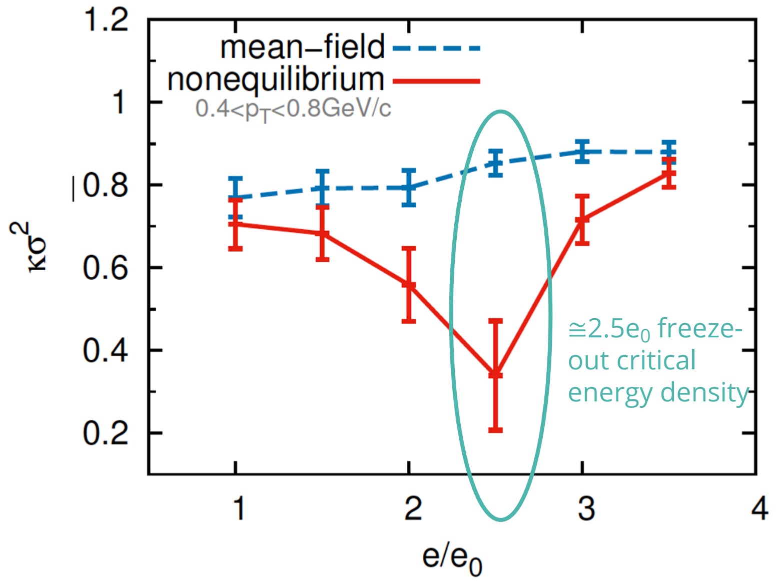

Lattice spacing dependence in simulations has been treated by coarse-graining the noise. We try to improve the approach with proper renormalization

Relaxation Model

Decouple the equations and consider a simpler model:

Stochastic Relaxation Equation

$$\frac{\partial^2 \varphi(\vec{x},t)}{\partial t^2} - \nabla^2 \varphi(\vec{x},t) + \eta \frac{\partial \varphi(\vec{x},t)}{\partial t} + \frac{\partial V_{\text{eff}}[\varphi]}{\partial \varphi(\vec{x},t)} = \boxed{\xi(\vec{x},t)}$$

Effective potential

$$V_{\text{eff}}(\varphi) = \frac{1}{2}\varepsilon\varphi^2 + \frac{1}{4}\lambda\varphi^4$$

The noise ξ is defined by

$$\langle \xi(\vec{x},t) \rangle = 0$$

$$\langle \xi(\vec{x},t)\xi(\vec{x}',t') \rangle = 2\eta T\ \delta(\vec{x}-\vec{x}')\delta(t-t')$$

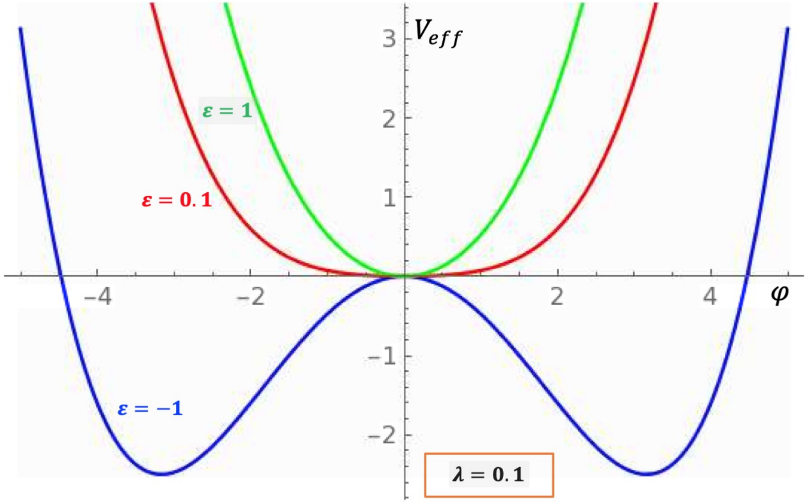

Lattice Spacing Dependence

➔ UV divergences caused by the noise translate as non-physical lattice spacing dependence in numerical simulations

$$\delta(\vec{x}' - \vec{x}) \to \frac{1}{dx^3}$$

➔ Loop corrections in the $\boldsymbol{\varphi}^4$ theory also introduce UV divergences

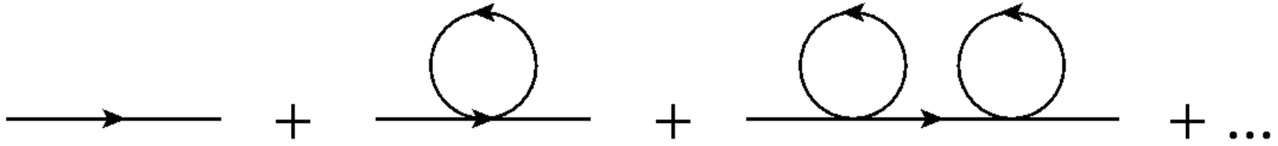

Jansen and Nickel

The tadpole diagram in the expansion of 2-point function gives a correction term (form depends on the regularisation/renormalization scheme)

Improved solution: lattice regularisation

Numerical simulations

- 3D system at fixed temperature: cubic lattice of sides *L=20 fm*, volume L^3
- N cells in each direction $\rightarrow$ Lattice spacing (use dx for simplicity)

$$dx = dy = dz = \frac{L}{N}$$

- Discretize time: repeat simulations for a number of time steps until equilibrium is reached
- Periodic boundary conditions
- Code on GPU: input equations and parameters ➞ evaluate the dynamical variable ➞ derive relevant observables (correlation function, different moments, etc.)

Linear Approximation of V_{eff} $(\varepsilon=1, \lambda=0)$

Consider system without interactions

The 2-point function is

$$C(r) = \frac{T}{4\pi r} e^{-\frac{r}{r_c}}$$

Correlation length

$$r_c = \sqrt{1/\epsilon} \quad r = |\vec{x} - \vec{x}'|$$

- Reproduced analytic result
- Benchmarked correlation function in our code
- No dx dependence for finite distances: introduced close to 0

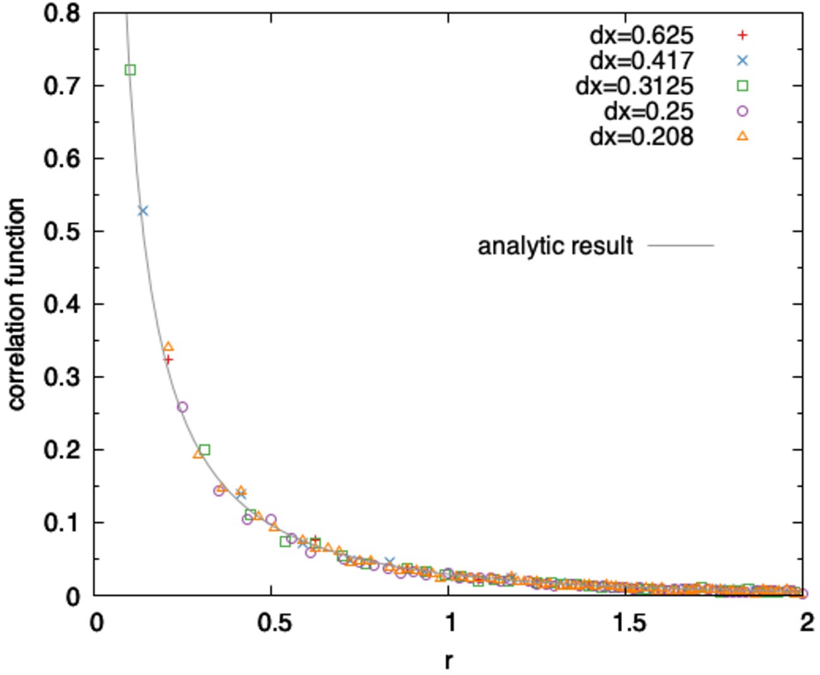

Linear Approximation of V_{eff} $(\varepsilon=1, \lambda=0)$

Integrate correlation function in 1d to benchmark a logarithmic dx dependence

$$C_{int} = \int_{dx}^{X} \frac{T}{4\pi r} e^{-\frac{r}{r_c}}\, \mathrm{d}r =$$

$$\frac{T}{4\pi} \int_{dx}^{X} \left(\frac{1}{r} - \frac{1}{r_c} + \frac{r}{2r_c^2} - \frac{r^2}{3!r_c^3} + \ldots\right) dr =$$

$$\frac{T}{4\pi} \left[ln(r) - \frac{r}{r_c} + \frac{r^2}{4r_c^2} - \frac{r^3}{18r_c^3} + \ldots \right]_{dx}^{X}$$

- Reproduced analytic result
- Benchmarked dx dependence

➡include nonlinear terms

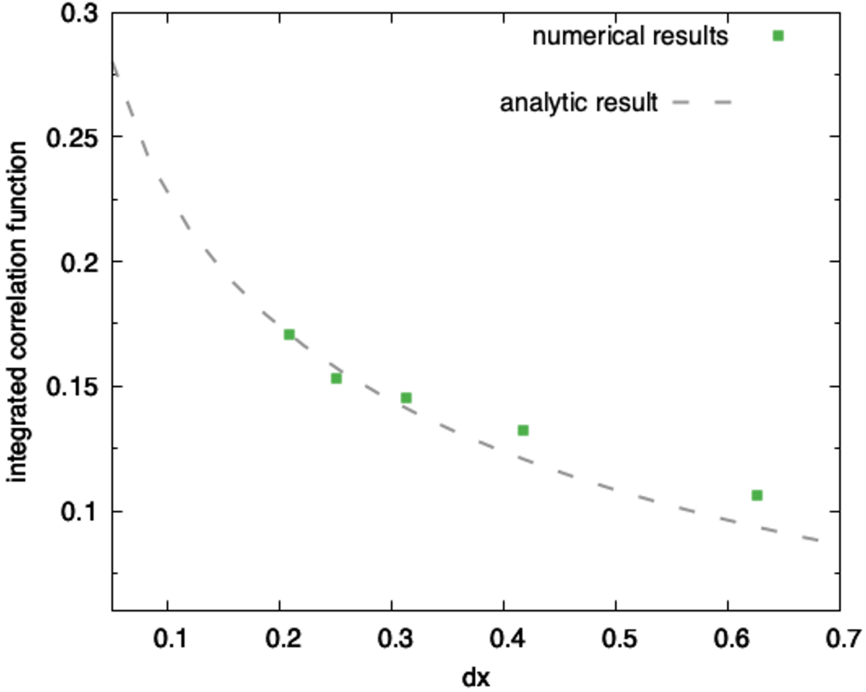

Observables: Mean and Variance

➔ Mean

$$\langle \varphi_V(t) \rangle = \frac{1}{V} \int d^3x \varphi(\vec{x}, t)$$

We are interested in fluctuation observables

➔ Variance

$$\langle \varphi_V^2(t) \rangle = \frac{1}{V} \int \int d^3x_1 d^3x_2 C(\vec{x_1} - \vec{x_2})$$

Where

$$X \leq \frac{L}{2} \Rightarrow V \propto V_{sphere}$$

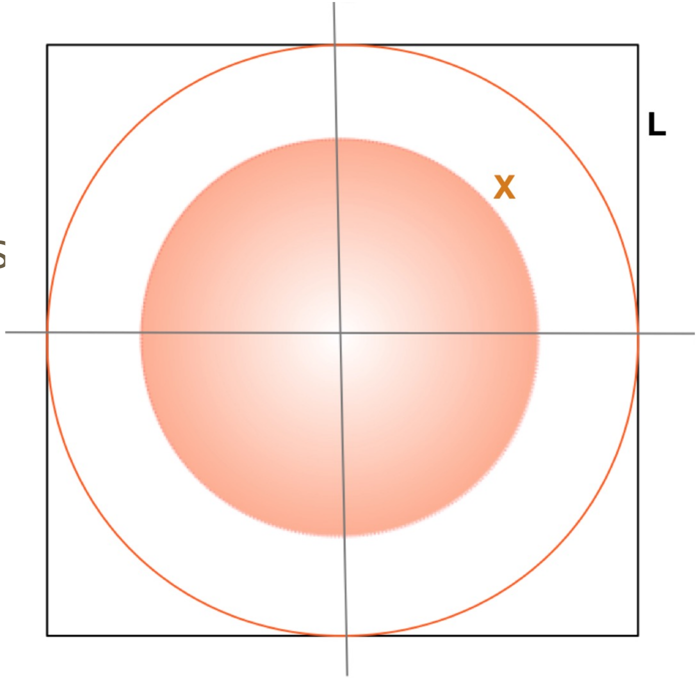

Mean and Variance at Equilibrium *ε=-1 λ=0.1* Broken Symmetry

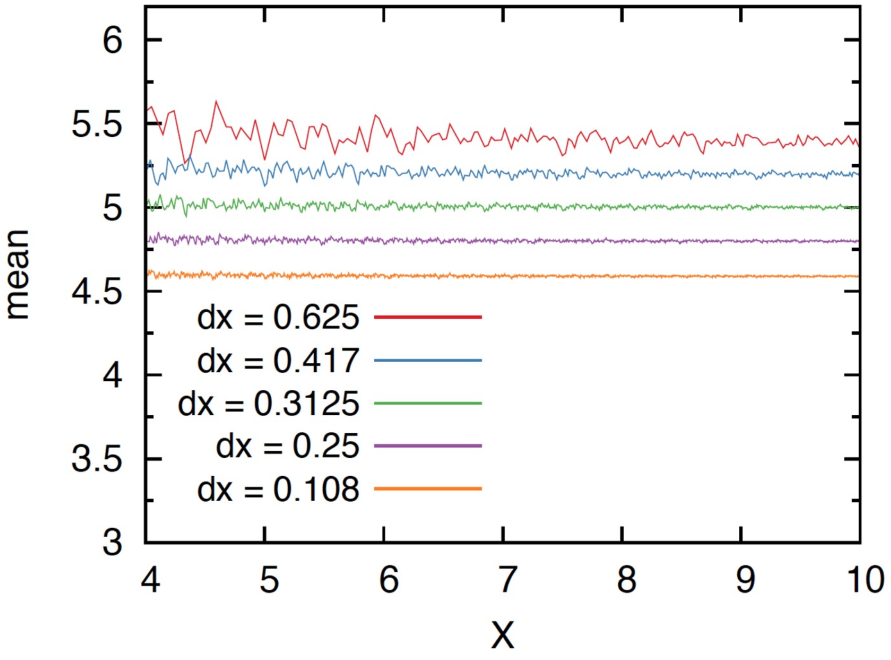

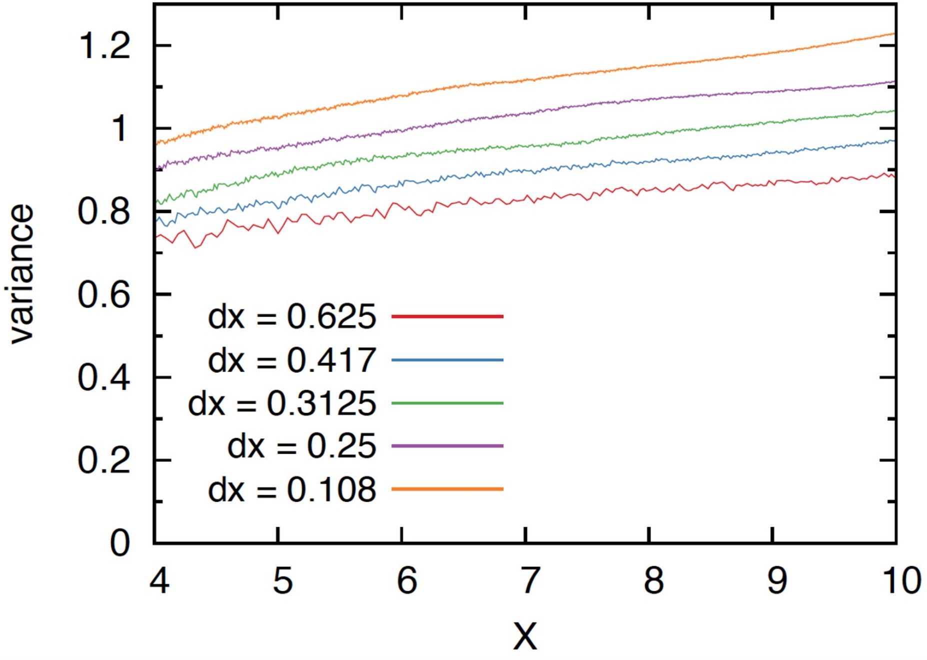

Both observables are clearly dx dependent

Lattice Regularisation

Equilibrium counterterm to correct V_{eff} from mass renormalization procedure

$$\mathcal{V}_{ct} = \{-\frac{3\lambda\Sigma}{4\pi}\frac{T}{dx} + \frac{3\lambda^2 T^2}{8\pi^2}[ln(\frac{6}{dxM}) + \zeta]\}\frac{\varphi^2}{2}$$

Cassol-Seewald et al. 0711.1866
Farakos et al. 9412091, 9404201v1
Gleiser, Ramos 9311278v

- Σ≈3.1759, ζ≈0.09
- M renormalization scale
- Leading 1/dx dependence

Equilibrium and dynamical evolution, with and without counterterm, for

- ε=-1 (broken symmetry)
- ε=0.1 (close to critical point)
- λ=0.1and λ=0.25
- T=M=η=1
- All quantities are dimensionless

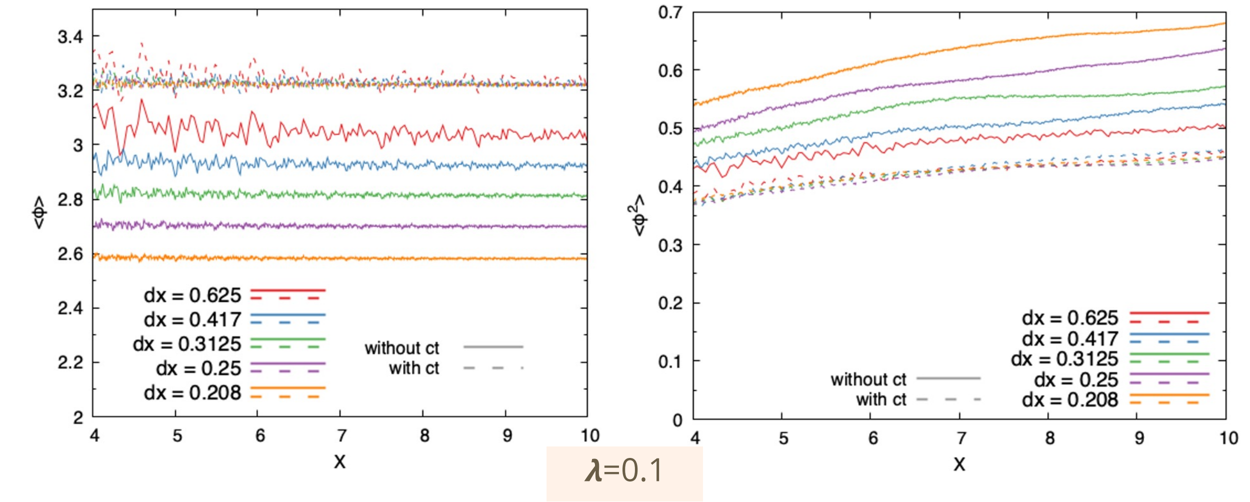

λ=0.1

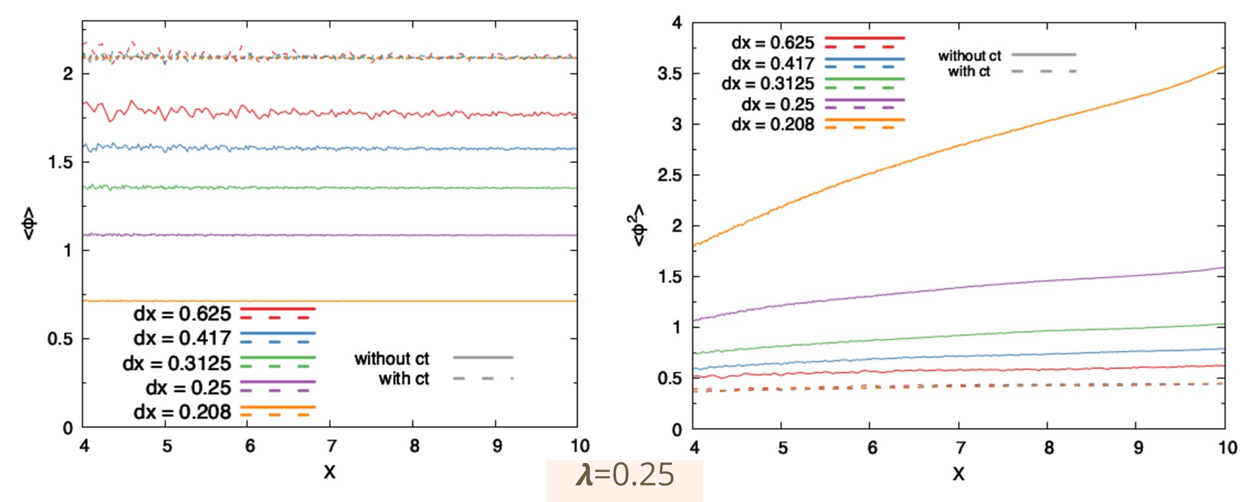

λ=0.25

Equilibrium

ε=-1 Broken Symmetry

Lattice spacing dependence corrected by the same counterterm

Consistent with previous equilibrium results for the mean

(Cassol-Seewald et al. 0711.1866 and references therein)

Equilibrium ε=0.1 close to Critical Point

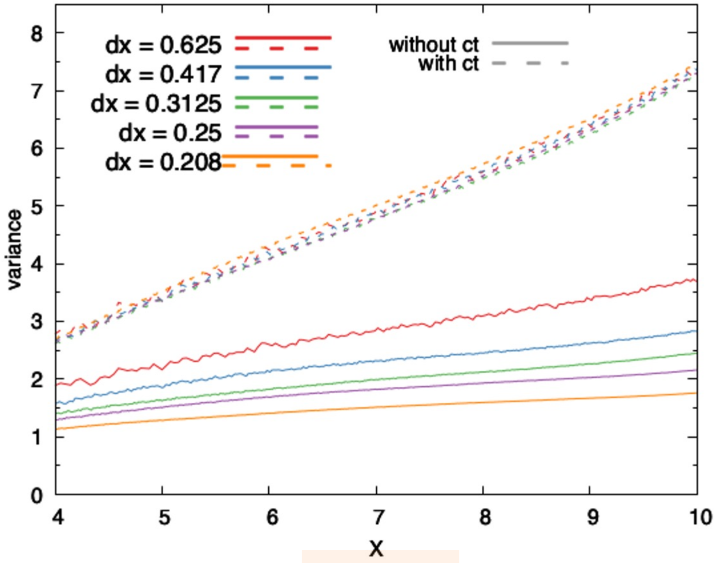

λ=0.1

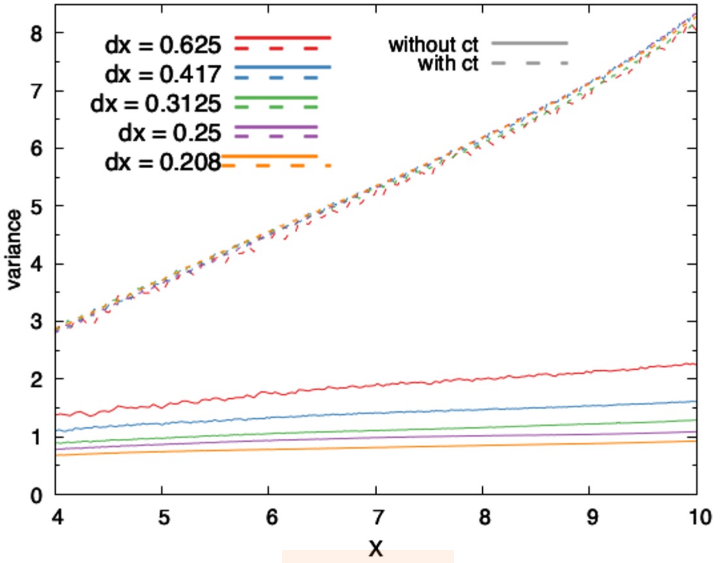

λ=0.25

Close to the critical point, as ε decreases, the correlation length diverges $r_c = \sqrt{1/\epsilon}$
Long-range fluctuations add up and the variance increases with the volume

Same counterterm corrects lattice spacing dependence close to critical point

Time Evolution ε=-1

Broken Symmetry

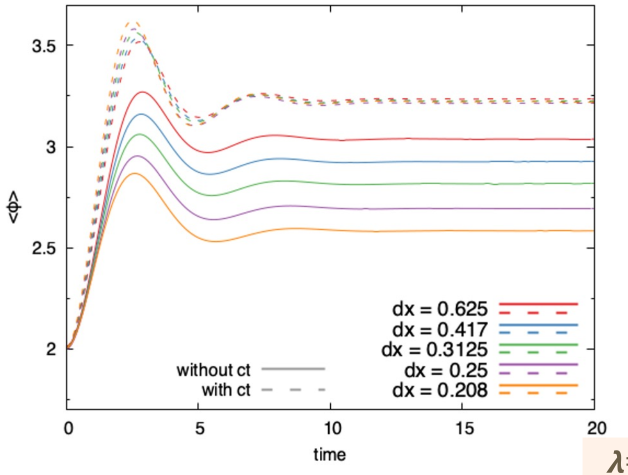

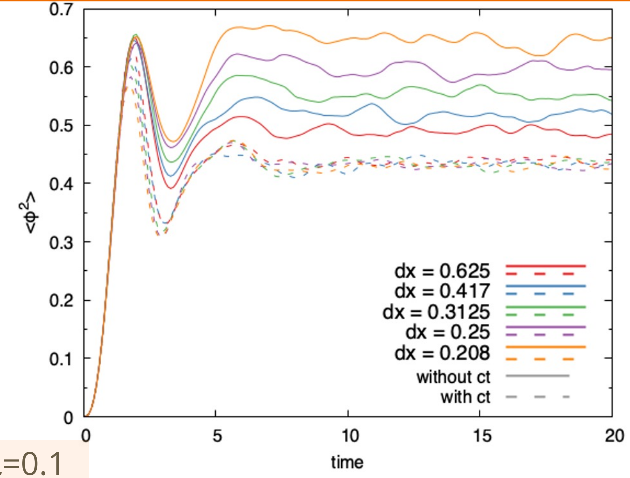

λ=0.1

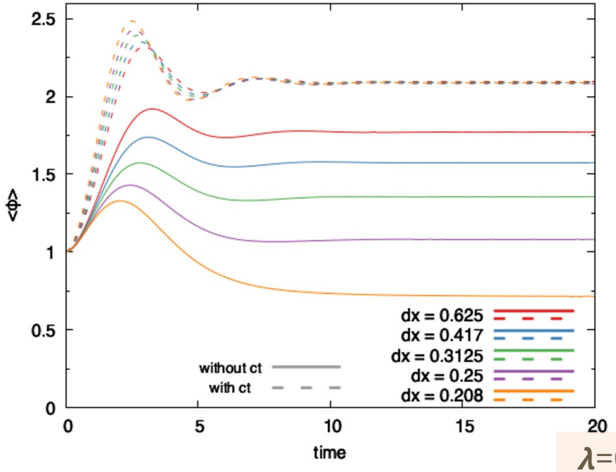

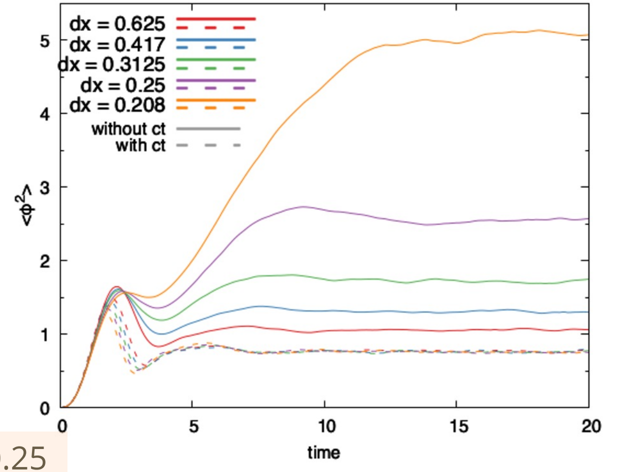

λ=0.25

At early times and despite being evaluated in equilibrium conditions, the counterterm significantly alleviates the dx dependence

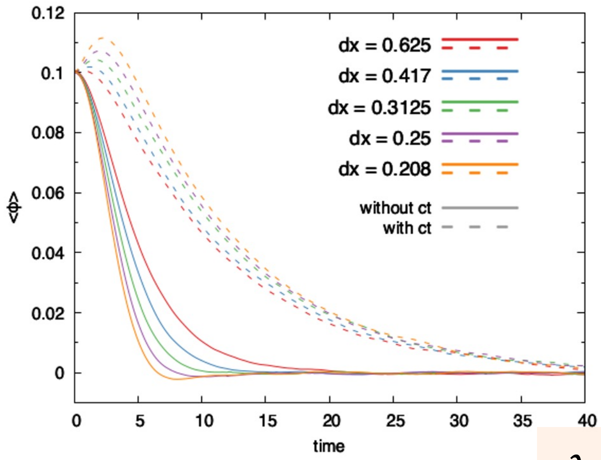

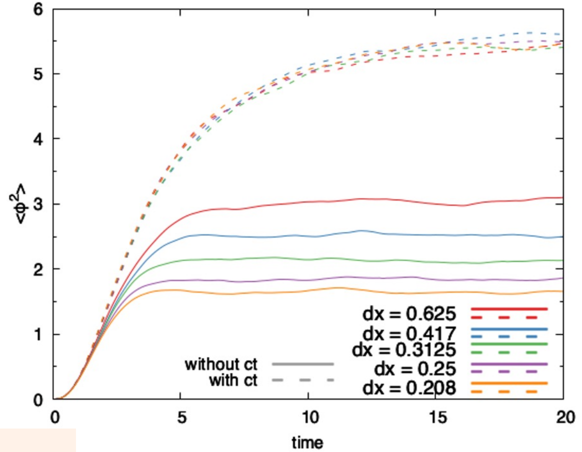

λ=0.1

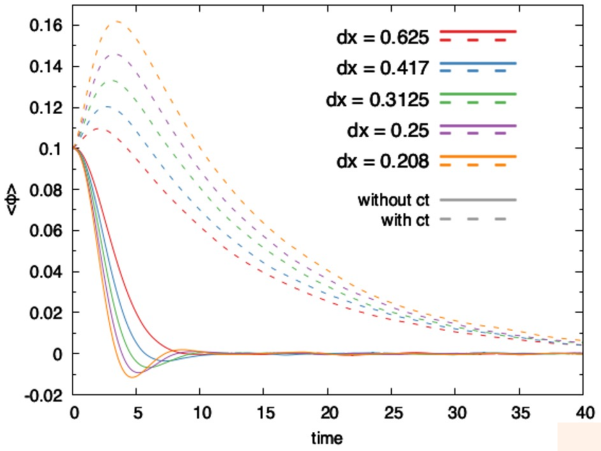

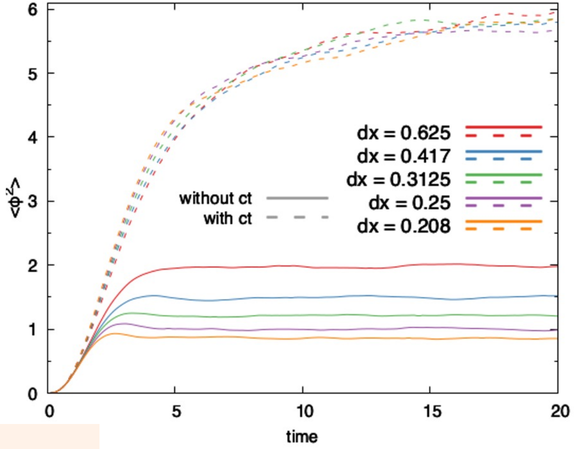

λ=0.25

Time Evolution

ε=0.1 close to Critical Point

Close to the critical point, the mean retains sensitivity to dx, takes longer to equilibrate and shows a qualitative change in behavior

The variance shows significant improvement

➜ Improve Renormalization (η, dynamic counterterm…)

Carbon footprint

- Numerical calculations were carried out on GPUs at the in2p3 computing center
- Number of GPU usage hours → TDP (thermal design power) of GPU to evaluate energy consumption → average CO_2/kWh in France for 2022

Cautious estimate between 325 and 390 $KgCO_2 eq$

For results shown here

➔ Average household emissions per month in France 22 $KgCO_2 eq$
➔ Average flight Nantes-Paris emissions per passenger 65.3 $KgCO_2 eq$
➔ My train ride from Nantes to Strasbourg 2.3 $KgCO_2 eq$
➔ Issues with accuracy of estimate

Summary and Outlook

- Properly benchmarked the fluctuations in the code
- Shown lattice spacing dependence of mean and variance
- Same counterterm works in equilibrium for mean and fluctuations both in the vicinity of the critical point and in the broken symmetry phase
- More work needed to understand effect of counterterm on dynamical evolution especially close to the critical point

➔ Dynamics for chiral field (V_{eff} and possibly η) in decoupled system first
➔ Apply approach to the coupled chiral fluid dynamics: derive proper counterterm(s)
➔ Apply approach using realistic initial conditions for HIC and equation of state of QCD

Backup: parameter file

```
Param(
  actions: [
    (Moments(["sig"]), TotalInterval(from: 0, to: 60, total: 1000)),
    (Window(["sig"]), At(60)),
    (StaticStructureFactor(["sig"], Radial), At(60)),
    (Correlation(["sig"],Radial), At(60)),
  ],
  config: (t_0: Some(0), t_max: 60, dim: D3S((32,20))),
  integrator: RK4(dt: 8.0000e-04),
  noises: Some([Normal(name: "xi")]),
  symbols: [
    "eta = 1
    eps = -1
    lam = 0.1
    T = 1
    sig' = psi
    psi' = #^2 sig - eta*psi - eps*sig -lam*sig^3 - sqrt(2*eta*T*ivdxyz*ivdt)*xi
    *sig = 0.1",
  ],
)
```

Backup: coarse-graining and filtering noise

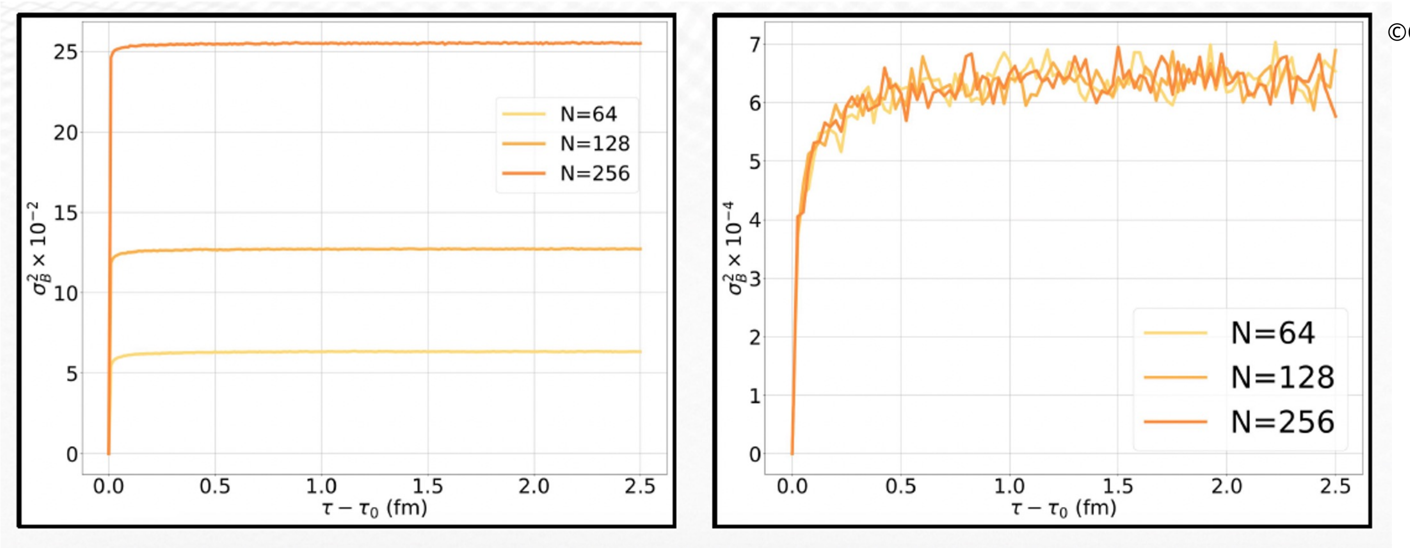

- ➢ Coarse-graining over grid of same scale
- ➢ Filtering large momenta modes in Fourier space
- ➢ Smearing by a Gauss distribution

2001.08831v1 [nucl-th] and references therein, 1704.03553

$$l_{grid} < l_{filter} \lesssim l_{hole} \ll l_{hydro}$$

Backup: some equations

3d integral of correlation function in linear approximation

$$\int \frac{T}{4\pi r} e^{-\frac{r}{rc}} d\vec{r} = \frac{T}{4\pi} \int_{dx}^{X} \int_{0}^{\pi} \int_{0}^{2\pi} \frac{r^2 sin\theta}{r} e^{-\frac{r}{rc}} dr d\theta d\phi = T[(dx + r_c)e^{-\frac{dx}{rc}} - (X + r_c)e^{-\frac{X}{rc}}]$$

Volume of integration sphere

$$\frac{L}{2} < X < \frac{L\sqrt{3}}{2} \Rightarrow V \propto \frac{4}{3}X^3 - 2\pi(X - \frac{L}{2})^2(2X - \frac{L}{2})$$

$$X = \frac{L\sqrt{3}}{2} \Rightarrow V = L^3$$